

NUMERICAL SIMULATION OF PITTING CORROSION

Alessandra Ferreira¹
Ivan Napoleão Bastos²
Antônio J. Silva Neto³

Instituto Politécnico, IPRJ, Universidade do Estado do Rio de Janeiro, UERJ, P.O Box 97282, 28601-970, Nova Friburgo RJ, Brazil
e-mail ¹afferreira@iprj.uerj.br, ²inbastos@iprj.uerj.br, ³ajsneto@iprj.uerj.br

Abstract. *In the present work a computational model of the pitting corrosion process is implemented. The mass transfer phenomena are modeled by a transient diffusion equation taking into account the competing mechanisms of accumulation of chloride ions and removal of such ions to the electrolyte. It is also taken into account the phenomenon of breakdown-repair, being mathematically modeled by an ordinary differential equation. The generation of pits over a metallic surface is modeled using a random nucleation process, and then the solution of the mathematical model provides a visualization of the surface damage.*

Keywords: *pitting corrosion, numerical simulation and stainless steel.*

1. Introduction

In recent years the pitting corrosion of metallic alloys has attracted the attention of several researchers, and most of the work performed has had an experimental approach. The complexity of the phenomena involved motivates new investigations on this type of localized corrosion since the technological problems related to pitting still persist. It is observed though that computer simulation of pitting corrosion has been less used in this field, albeit the interesting new insights the simulation can provide to materials science as a whole.

Pitting corrosion takes place in metals immersed in electrolytes that promote passivation, such as stainless steel in several environments. When this occurs, an oxide film is formed. Several agents, such as mechanical scratch, high chloride concentration, acidity, high electrochemical potential, among others, can destroy the stability of this film, and a pit begins its nucleation.

The pitting events are generally believed to be stochastic, and statistical distributions are used to model the behavior of pitting (Shibata, 1996). The occurrence of pitting clusters has experimental evidence (Harlow and Wei, 1998), even affecting the mechanical resistance of structures such as pipelines (Chouchaoui and Pick, 1996). This behavior suggests that there are interactions occurring amongst the pits.

All commonly used stainless steels, which are designed to be corrosion-resistant, may be affected by pitting corrosion. Pitting corrosion presents a non-linear behavior, with a sharp rise in the corrosion rate even with a small change in the local environment in which the material is immersed. This mechanism may lead to the failure of a structure or damage of industrial equipment with possible loss of lives and high economic costs. The susceptibility of passive metallic alloys to pitting attack is dependent on the concentration of aggressive ions, such as chlorides.

Recently Malki and Baroux (2005) presented a computer simulation of the pit growth performed using both Monte Carlo and Cellular Automata techniques. Each part of metal/film/electrolyte is considered a cell that changes its states according to rules that depend on the initial state and the effect of neighboring cells. In their study an important role is found to be related to the IR drop, *i.e.*, ohmic drop inside the pit. Based on their results, when the IR is different from zero, the pit grows. Besides that, each cell is sensitive to the neighbor cells, but the influence of each pit is of short spatial range.

The susceptibility of pitting is dependent on several factors, such as electrochemical potential, ohmic drop, chloride content, temperature, non-metallic inclusions, dissolved oxygen, mass transport, and so on. Some of them have a clear deterministic action, as is the case of MnS inclusions in stainless steel (Schmuki et al., 2005, Budianski et al., 2004). In this case pit always starts nucleation at the interface between the MnS inclusion and the base stainless steel. With such highly complex situation it is reasonable to try to develop mathematical models based on a phenomenological approach. One of the most interesting models already proposed takes into account the spatio-temporal interactions of pits (Punckt et al., 2004). This model has deterministic and stochastic assumptions that affect both the generation and growth of pits. However, the model needs to be further tested and improved, mainly in the feedback effects after the occurrence of pitting. Despite this fact, it allows the numerical simulation of many factors that are fully established in practice. Thus, the model is robust enough to simulate several real situations.

In the present paper a computational model for pitting corrosion mechanism with some variations with respect to other models already published (Punckt et al., 2004; Lunt et al., 2002, Brusamarello, 2003) is performed. One modification is the elimination of ohmic drop near the surface. This situation is expected to occur in electrolyte with high chloride content, of approximately one molar. Therefore, the electrical conductivity is high and the product IR is negligible (Engelhardt and Macdonald, 2004). Another modification implemented in the model is that the behavior law for pit generation is initially completely random, but after each nucleation a feedback mechanism takes place and the

rearranging of chloride diffusion around each pit modifies the original probability law. The mathematical model and results for the numerical simulation are presented.

2. Mathematical formulation of the pitting corrosion phenomenon

The mathematical model developed in the present work for pitting corrosion mechanism is based on the model developed by Punckt et al. (2004).

The local concentration of aggressive species in the diffusion boundary layer can be calculated with

$$\frac{\partial c}{\partial t} = -\gamma c + D \nabla^2 c + \sum_i S(t-t_i) \quad (1)$$

where c represents the ion concentration, γ the rate constant for the loss of aggressive species due to its diffusion into the bulk of the electrolyte in which the metal under analysis is immersed, D is the diffusion coefficient related to the lateral diffusion of the ions within the diffusion boundary layer, and $\sum_i S(t-t_i)$ represents a source term associated with the pits which are generated at the activation times represented by t_i , with $i = 1, 2, \dots, N_g$, and N_g is such that t_{N_g} is less than the final time of observation t_f .

In Eq. (1) the rate constant is expressed as

$$\gamma = \frac{2D}{l_o^2} \quad (2)$$

where l_o is the thickness of the diffusion boundary layer.

In the present work the aggressive ions are chloride, but in more complex situations other types of chemical species may be considered, such as metallic ions and dissolved oxygen besides the chloride. Equation (1) describes how the chloride ion is distributed on the metallic surface as a function of time. As mentioned before the first term on the right hand side (RHS) of Eq. (1) models the loss of chloride ions to the bulk of the electrolyte. The second term on the RHS models the lateral diffusion of the chloride ions within the diffusion boundary layer. The source term, i.e., the third term on the RHS of the Eq. (1), is activated when a pit occurs. In order to maintain the local electroneutrality more chloride is then attracted to the pit site. The source term is mathematically modeled as

$$S(t-t_i) = \frac{AK}{l_o} g(t-t_i) \delta(\vec{r} - \vec{r}_i) \quad (3)$$

where A is a constant that was included in the model just to allow the control on the influence of the source term, K represents the number of moles of the aggressive ions liberated by an active pit during its lifetime, \vec{r} is the spatial coordinate and \vec{r}_i represents the location of a pit. In the present work a slightly more general formulation is allowed in which at the same time a group of pits can be activated simultaneously, and therefore \vec{r}_i represents the location of all pits generated at the same time which will be accounted for simultaneously as the group of pits with index i , and the time of activation t_i . In the present work an exponential decay of the pit with time is considered, i.e.

$$g(t-t_i) = \begin{cases} \frac{1}{\tau_0} \exp\left(-\frac{t-t_i}{\tau_0}\right), & t > t_i \\ 0, & t < t_i \end{cases} \quad (4)$$

where τ_o is the lifetime of a pit (i.e. of a group of pits). Observe that in the present model all pits are considered identical because their lifetime τ_o and maximum value (at $t = t_i$) given by $\frac{AK}{l_o \tau_o}$ are all identical.

The passive film of oxide is affected by the concentration of aggressive ions, but in their absence the oxide film is able to repair itself. In the model of Punckt et al. (2004), a phenomenological variable s is then introduced as a measure of local film damage. Considering a linear variation of the rate of change of s with the chloride concentration and a linear dependence with the level of damage results

$$\frac{\partial s}{\partial t} = -k s + \nu c \quad (5)$$

where k is the rate constant for the repassivation phenomenon and ν is the rate constant for the film breakdown. The recovery time of the oxide layer is

$$T_o = \frac{1}{\nu} \quad (6)$$

In the model developed by Punckt et al. (2004) the local generation rate of active pits w increases with the concentration of the aggressive species c and with the level of damage s in the oxide film, but is reduced with the local ohmic potential drop ϕ which has a short range effect, as follows

$$w(c, s) = \frac{w_{\max}^R}{1 + \exp\left[\frac{M_0 - \alpha_c c - \alpha_s s + \alpha_\phi \phi}{H}\right]} \quad (7)$$

where w_{\max}^R is the saturation value, M_0 is a threshold value at which a steep increase of the pitting rate occurs, H determines how steep this increase is, and α_c determines the influence of the aggressive ion concentration, α_s the influence of the level of film damage and α_ϕ the influence of the ohmic potential drop, respectively, in the rate of pit generations.

The rate of spontaneous pit generation for a damage-free film ($s = 0$) in the absence of aggressive ions ($c = 0$) is given by

$$w_0 = \frac{w_{\max}^R}{1 + \exp\left(\frac{M_0}{H}\right)} \quad (8)$$

As a variation in the model developed by Punckt et al. (2004), the following normalization is used

$$w' = \frac{w - w_{\min}}{w_{\max} - w_{\min}} \quad (9)$$

such that $0 \leq w' \leq 1$, where w_{\max} and w_{\min} are the maximum and the minimum values, respectively, calculated for w in the whole spatial domain at each time t in the period of observation $0 \leq t \leq t_f$. A random number p is then generated in the range $[0,1]$. If $p < w'$ a pit is generated in a randomly chosen location \vec{r}_i , yielding the source term as given by Eqs. (3) and (4). Another change is introduced in the original model in order to allow the generation of stable pits. A second normalization was used in order to deal separately with the occurrences of stable and non-stable pits,

$$s' = \frac{s - s_{\min}}{s_{\max} - s_{\min}} \quad (10)$$

such that $0 \leq s' \leq 1$, where s_{\max} and s_{\min} are the maximum and minimum values, respectively, calculated for s in the whole spatial domain at each time t in the period of observation $0 \leq t \leq t_f$. A random number q is then generated in the range $[0,1]$. If $(q + \beta) < s'$ a pit generated in location \vec{r}_i has its strength set to the maximum value $\frac{AK}{l_o \tau}$ and it is kept constant for all times $t_i \leq t \leq t_f$, i.e., it is not allowed to decay exponentially with time as happens with the other pits modeled with Eqs. (3) and (4). The parameter β was added to the random number q in order to allow a better control on the number of stable pits.

3. Numerical solution

In the present analysis a steel plate with dimensions $L_x \times L_y$ is considered, as shown in Fig. 1.

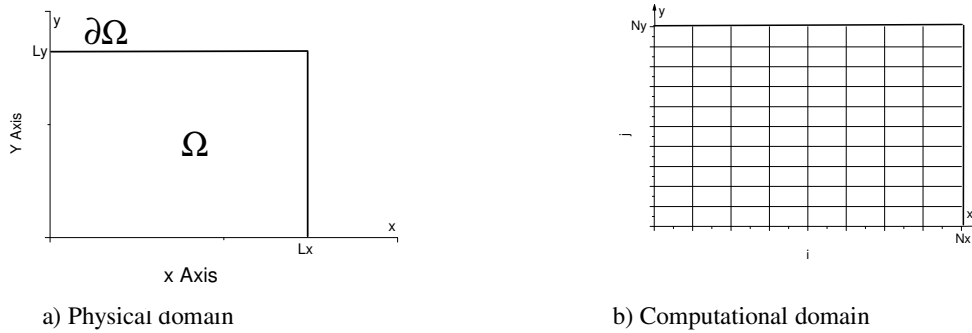


Figure 1. Physical and computational domains.

The mathematical model described in the previous section is then written for the two-dimensional domain represented in Fig. 1,

$$\frac{\partial c(x, y, t)}{\partial t} = -\gamma c(x, y, t) + D \left[\frac{\partial^2 c(x, y, t)}{\partial x^2} + \frac{\partial^2 c(x, y, t)}{\partial y^2} \right] + F(i, t_i, w', s') \text{ in } \Omega \text{ and } \Gamma \quad (11)$$

$$\frac{\partial s(x, y, t)}{\partial t} = -k s(x, y, t) + \nu c(x, y, t) \text{ in } \Omega \text{ and } \Gamma \quad (12)$$

$$w(x, y, t) = \frac{w_{\max}^R}{1 + \exp[(M_o - \alpha_c c(x, y, t) - \alpha_s s(x, y, t)) / H]} \text{ in } \Omega \text{ and } \Gamma \quad (13)$$

where

$$\Omega = (0, L_x) \times (0, L_y) \text{ and } \Gamma = [0, t_f] \quad (14)$$

In Eq. (11) F represents the source term given by Eqs. (3) and (4) taking into account the following feedback mechanisms: (i) the probability of generating a pit increases with the increasing value of w ; and (ii) the pit will be stable depending on the value of s . These mechanisms were described in the previous section, and will not be repeated here. By comparing Eqs. (7) and (13) one can observe that the effect of the ohmic potential drop was neglected. This

effect will be investigated in future works. In order to solve Eqs. (11) and (12) a set of the initial and boundary conditions is needed. In the present work the following conditions are considered

$$c(x,y,t) = 0 \quad \text{in } \Omega, \quad \text{for } t=0 \quad (15)$$

$$s(x,y,t) = 0 \quad \text{in } \Omega, \quad \text{for } t=0 \quad (16)$$

$$c(x,y,t) = 0 \quad \text{in } \partial\Omega, \quad \text{for } 0 \leq t \leq t_i \quad (17)$$

An explicit finite difference approximation was developed for the problem described by Eqs. (11–17), being used the computational domain represented in Fig. 1(b). The computation of the source term F in Eq. (11) was performed lagging the contributions of s and w by one time step. The following set of uncoupled equations is then obtained:

$$c_{i,j}^{n+1} = c_{i,j}^n + \Delta t \left\{ -\gamma c_{i,j}^n + \frac{D}{\Delta x^2} [c_{i-1,j}^n - 2c_{i,j}^n + c_{i+1,j}^n] + \frac{D}{\Delta y^2} [c_{i,j-1}^n - 2c_{i,j}^n + c_{i,j+1}^n] + F(i,t_i, s^n, w^n) \right\},$$

$$i = 1, 2, \dots, Nx-1, j = 1, 2, \dots, Ny-1 \text{ and } n = 0, 1, \dots, N_t \quad (18)$$

$$s_{i,j}^{n+1} = s_{i,j}^n + \Delta t (-ks_{i,j}^n + vc_{i,j}^n), \quad i = 1, 2, \dots, Nx-1, j = 1, 2, \dots, Ny-1 \text{ and } n = 0, 1, \dots, N_t \quad (19)$$

$$w_{i,j}^n = \frac{w_{\max}^R}{1 + \exp[(M_o - \alpha_c c_{i,j}^n - \alpha_s s_{i,j}^n) / H]},$$

$$i = 1, 2, \dots, Nx-1, j = 1, 2, \dots, Ny-1 \text{ and } n = 0, 1, \dots, N_t \quad (20)$$

$$\Delta t = \frac{t_f}{N_t}; \quad \Delta x = \frac{L_x}{N_x}; \quad \Delta y = \frac{L_y}{N_y} \quad (21a-c)$$

Starting with the initial conditions $c_{i,j}^0 = s_{i,j}^0 = 0$, $i = 1, 2, \dots, Nx-1$, $j = 1, 2, \dots, Ny-1$ a forward sweep is performed in the discretized time domain $n = 0, 1, \dots, N_t$, with Eqs. (18–21) yielding the values of c , s and w . A description of the procedure to be used to calculate the source term F in Eq. (18) was given in the previous section.

4. Results and discussion

Several test cases were performed in order to investigate the behavior of the pit corrosion model described in Sections 2 and 3. In Table 1 are presented the reference values for the parameters. Most of them were extracted from Punckt et al. (2004).

Before the presentation of the computational results of the model, the generation of the first two groups of pits is shown. They are generated according to the pits density prescribed by the Standard Practice ASTM G46-92 (1993). A density of 5 pits/cm² was used. Other values will be investigated in future works. At each time step a group of pits may be generated. As shown in Fig.2 the first two groups of pits were generated at $t = 0.1$ s and 0.3 s. No new pits were generated at $t = 0.2$ s. In Fig. (2b) it can be observed that the first group of pits is already decaying when the second group of pits is generated. After the first two groups of pits are generated, new pits may be generated according to the normalized values w' and s' as given by Eqs. (9) and (10), respectively, using the procedure described at the end of Section 2. In Fig. 3 are shown the contour plots for c , s and w , at three different times: 0.5 s, 4.5 s and 9 s. An aggressive condition in which after 9 s a severe damage is already observed in the material was considered in the simulated test cases.

In Fig. 4 are shown the countour plots for c , s and w at the time $t=9$ s, considering three different values for the parameter A in Eq. (3). This parameter was arbitrarily introduced in order to analyse the effects of the intensity of the source. It is also shown the location of the pits. A strong pit density is observed in Fig. 4c in which the intensity of the source is the highest.

In Fig. 5 are shown the contour plots for c , s and w at the time $t = 9$ s, considering two different values for the diffusion coefficient D . In Fig. 5(a) it is considered $D = 1.0 \times 10^{-7}$ cm²/s and in Fig. 5 (b) $D = 1.0 \times 10^{-5}$ cm²/s.

From Fig. 5 one can observe that, as expected, when the lateral diffusion coefficient is reduced, the damage to the oxide film is more restricted to the area closer to the pits. As it increases the damage reaches a larger area.

Table 1 – Reference values for the parameters used in the computational model of the pitting corrosion.

Parameter	Equation or Section	Value
γ	Eq. (1)	0.8 s^{-1}
D	Eq. (1)	$10^{-5} \text{ cm}^2 \text{ s}^{-1}$
t_f	Section 2	9 s
l_0	Eq. (2)	0.0005 cm
A	Eq. (3)	1.5×10^6
K	Eq. (3)	$2.1 \times 10^{-12} \text{ mol}$
τ_o	Eq. (4)	1 s
V	Eq. (5)	0.033 s^{-1}
w_{\max}^R	Eq. (7)	$10^3 \text{ mol}^{-1} \text{ cm}^3 \text{ s}^{-1}$
M_0	Eq. (7)	50
α_c	Eq. (7)	$8.78 \times 10^6 \text{ cm}^3 \text{ mol}^{-1}$
α_s	Eq. (7)	7210
α_ϕ	Eq. (7)	0
H	Eq. (7)	10
β	Section 2	0.3
L_x	Section 3	2.5 cm
L_y	Section 3	2.5 cm
N_x	Section 3	70
N_y	Section 3	70
N_t	Section 3	90
Δt	Eq. (21a)	0.1 s
Δx	Eq. (21b)	0.036 cm
Δy	Eq. (21c)	0.036 cm

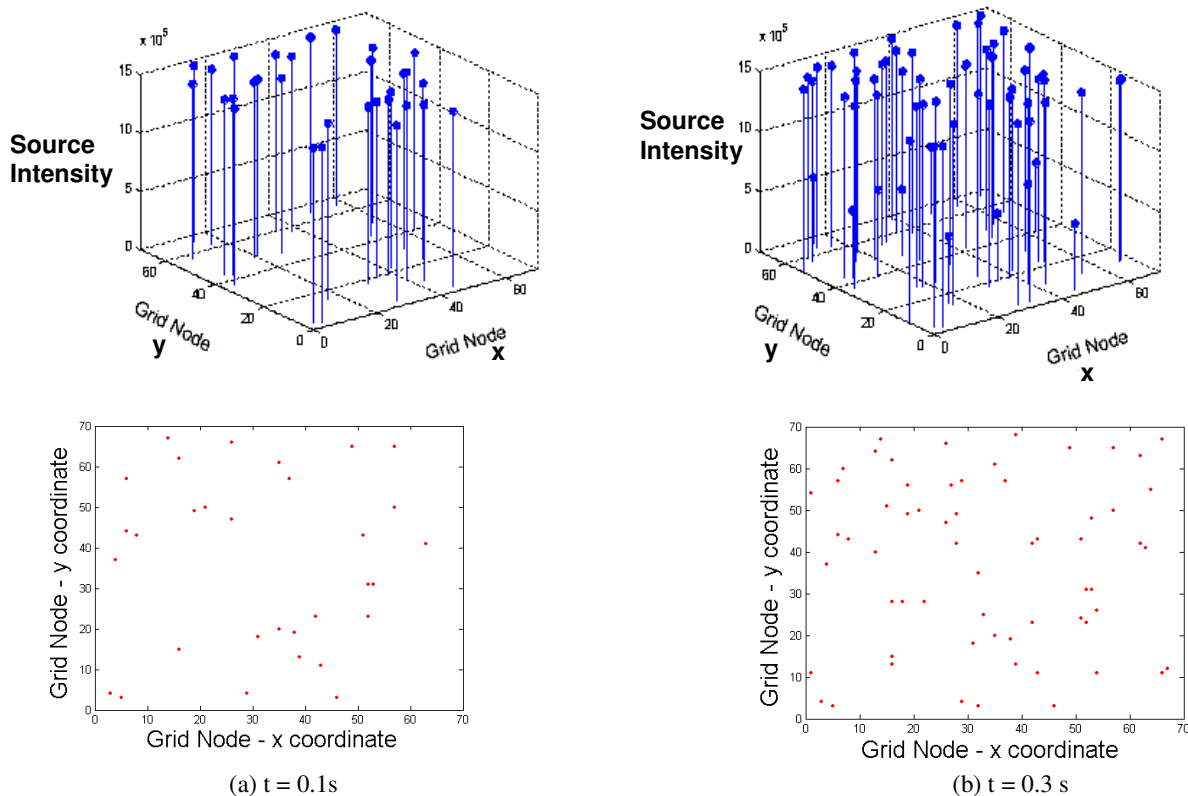


Figure 2 – Generation of the first two groups of pits.

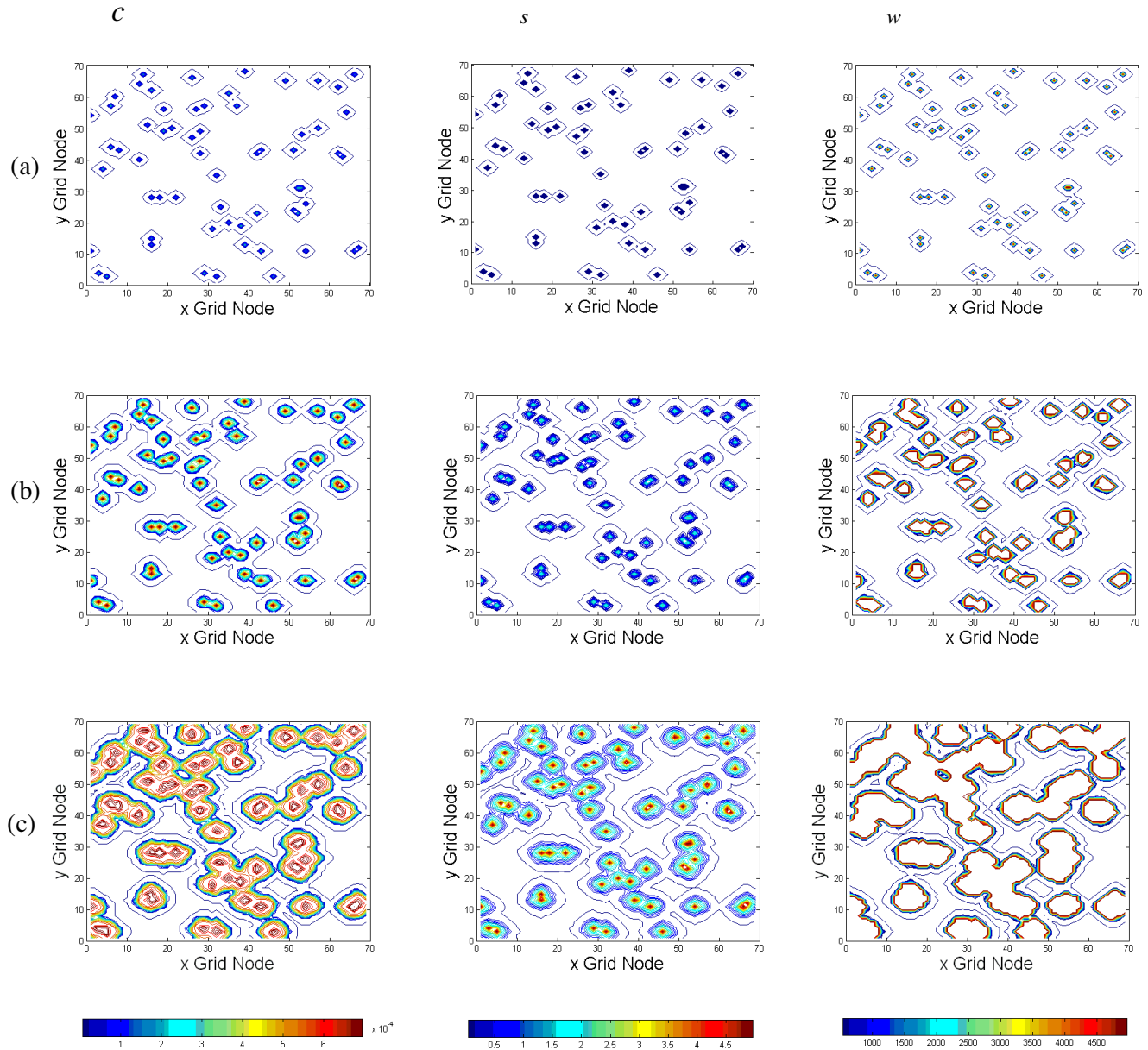


Figure 3 – Contour for c , s and w , at three different time steps: (a) $t = 0.5$ s, (b) $t = 4.5$ s and (c) $t = 9$ s

4. Conclusions

In this paper a simulation of the behavior of pitting corrosion applied to materials such as stainless steel exposed to an electrolyte with ions aggressive enough to breakdown the passivating layer was presented. The model takes into account the effects of interaction among neighbor pits, and considers as relevant phenomena the diffusion of aggressive ions, as chloride, on the metallic surface and to the electrolyte, the repassivation rate, and the degree of local film damage. Moreover, a modified phenomenological dependency law was used in order to generate the pits and as a consequence affect the spatio-temporal profiles of ion concentration, which for its turn affect the vicinity leading to the creation of cluster of pits, which have already been observed experimentally.

5. Acknowledgements

The authors acknowledge the financial support provide by CNPq, Conselho Nacional de Desenvolvimento Científico e Tecnológico and FAPERJ, Fundação Carlos Chagas Filho de Amparo à Pesquisa do Estado do Rio de Janeiro.

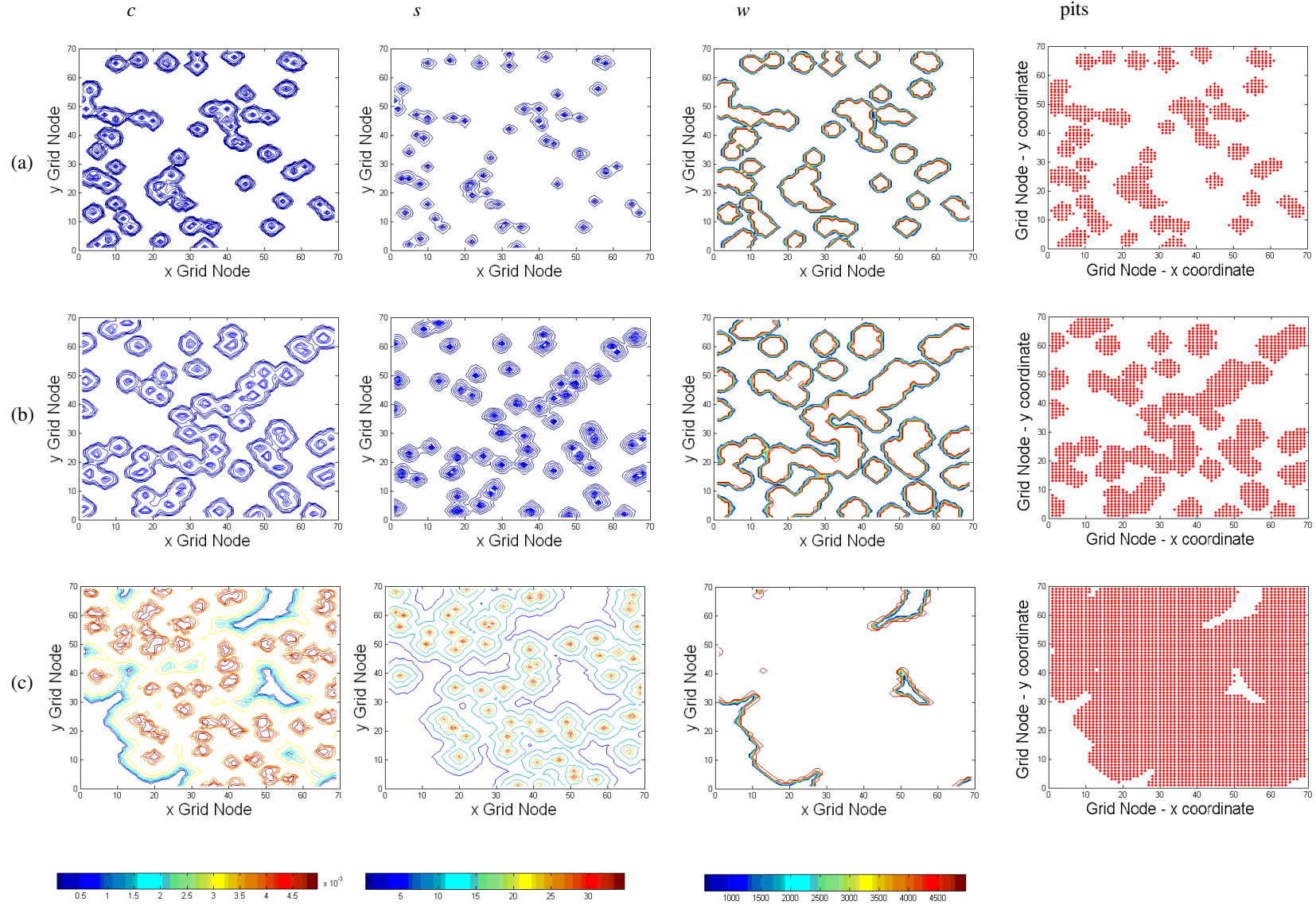


Figure 4 – Contour plot for c , s and w , and pit locations at $t = 9$ s as a function of parameter A (see Eq. 3): (a) $A = 1.0 \times 10^6$, (b) $A = 1.5 \times 10^6$ and (c) $A = 1.0 \times 10^7$

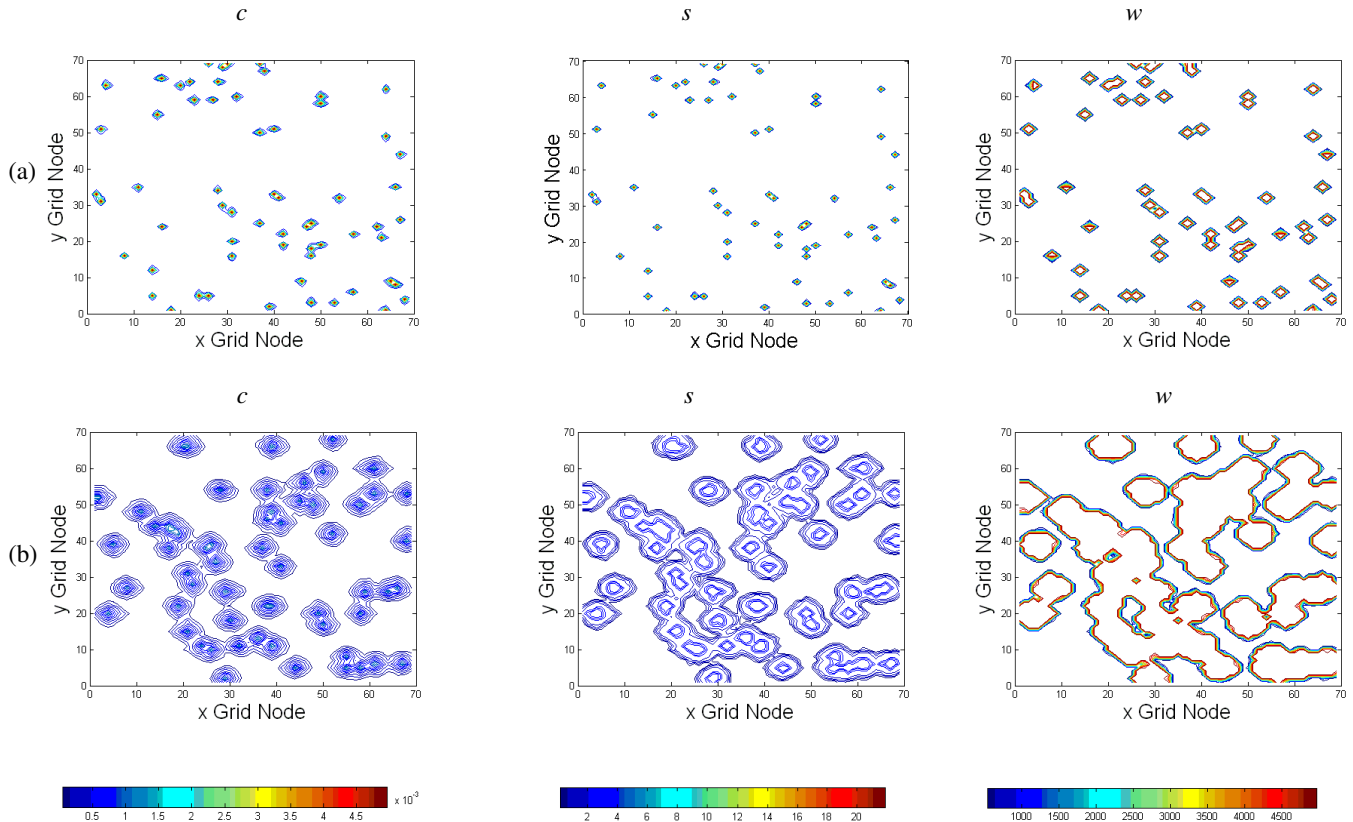


Figure 5 – Contour plot for c , s and w , as a function of the lateral diffusion coefficient:
(a) $D = 10^{-7} \text{ cm}^2/\text{s}$; (b) $D = 10^{-5} \text{ cm}^2/\text{s}$

6. References

- Brusamarello, V., 2003, "Simulation of Stable and Meta-Stable Pitting Process", Proceedings of the 7th Conference on Technology of Equipments, 7th COTEQ, Florianópolis, Brazil (in portuguese).
- Budianski, N. D., Hudson, J. L. and Scully, J. R., 2004, "Origens of Persistent Interaction Among Localized Corrosion Sites on Stainless Steel", Journal of the Electrochemical Society, Vol. 151, pp.B223-B243.
- Chouchaoui, B. A and Pick, R. J., 1996, "Behaviour of Longitudinally Aligned Corrosion Pits", Int. J. Ves. & Piping, Vol. 67, pp.17-35.
- Engelhardt, G and Macdonald, D. D., 2004, "Estimation of Corrosion Cavity Growth Rate for Predicting System Service Life", Corrosion Science, Vol. 46, pp.1159-1187.
- Harlow, D. G. and Wei, R. P., 1998, "A Probability Model for the Growth of Corrosion Pits in Aluminum Alloys Induced by Constituent Particles", Engineering Fracture Mechanics, Vol. 59, No.3, pp.305-325.
- Lunt, T. T., Scully, J. R., Brusamarello, V., Mikhailov, A. S. and Hudson, J. L., 2002, "Spatial Interactions Among Localized Sites, Experiments and Modeling", Journal of the Electrochemical Society, Vol.149, No.5, pp.163-B173.
- Malki, B. and Baroux, B., 2005, "Computer Simulation of Corrosion Pit Growth", Corrosion Science, Vol.47, pp.171-182.
- Punckt, C., Bölscher, M., Rotermund, H. H., Mikhailov, A. S., Organ, L., Budiansky, N., Scully, J. R. and Hudson, J. L., 2004, "Sudden Onset of Pitting Corrosion on Stainless Steel as a Critical Phenomenon", Science, Vol.305, pp.1133-1136.
- Standard Practice for Examination of Pitting Corrosion, ASTM G46-92, 1993, Annual Book of ASTM Standards, Section 3 Race Street, Philadelphia, USA.
- Shibata, T, 1996, "Statistical and Stochastic Approaches to Localized Corrosion", Corrosion, Vol.52, No.11, pp.813-829.
- Schmuki, P., Hildebrand, H., Friedrich, A and Virtanen, S., 2005, "The Composition of the Boundary Region of MnS Inclusions in Stainless Steel and its Relevance in Triggering Pitting Corrosion", Corrosion Science, Vol.47, pp.1239-1250.

7. Responsibility notice

The authors are the only responsible for the printed material included in this paper.